Structure–Property Relationships in Superconducting Cuprates

C. N. R. Rao*

Department of Chemistry, University of Wales, Cardiff CF1 3TB, U.K., and Solid State and Structural Chemistry Unit, Indian Institute of Science, Bangalore 560 012, India

A. K. Ganguli

CSIR Centre of Excellence in Chemistry, Indian Institute of Science, Bangalore 560 012, India

1 Introduction

The highest superconducting transition temperature known till 1986 was 23K and it seemed as though this barrier would not be broken.[1] The discovery of 30K superconductivity in an oxide of the La–Ba–Cu–O system by Bednorz and Müller[2] changed the picture. A variety of superconducting oxides, especially cuprates, have since been synthesized and characterized,[3–6] the highest transition temperature as of today being 155K in $HgBa_2Ca_2Cu_3O_{8+\delta}$. Studies of the various families of cuprates have shown many commonalities and unifying features.[6,7] Properties of the cuprates have been related to certain structural and electronic parameters. Although there is no simple relationship between the superconducting transition temperature and any specific structural feature of the cuprates, the various correlations help us to understand these materials better and to design newer ones. In this article, we shall briefly examine some of the significant structure–property relationships in superconducting cuprates along with the structural commonalities.

2 Common Structural Features

Many cuprate families have been discovered in the past seven years. The general features of the cuprates are shown schematically in Figure 1. The major families of cuprates are:
(a) $La_{2-x}A_xCuO_4$ (A = alkaline earth) possessing the K_2NiF_4(T) structure; (b) $LnBa_2Cu_3O_{7-\delta}$ (Ln = Y or rare-earth other than Ce, Pr, and Tb) referred to as the 123 type (Figure 2) and the related $LnBa_2Cu_4O_8$ (124) and $Ln_2Ba_4Cu_7O_{15}$ (247) cuprates containing perovskite layers with CuO_2 sheets as well as Cu–O chains; (c) $Bi_2(Ca,Sr)_{n+1}Cu_nO_{2n+4}$ containing two BiO layers and perovskite layers with CuO_2 sheets (Figure 2); (d) $Tl_2A_{n+1}Cu_nO_{2n+4}$ and $TlA_{n+1}Cu_nO_{2n+3}$ (A = Ca, Ba, Sr *etc.*) containing Tl–O layers and perovskite layers with CuO_2 sheets (Figure 2); (e) lead-based superconducting cuprates such as $Pb_2Sr_2LnCu_3O_8$ containing CuO_2 sheets and CuI–O sticks; (f) Tl, Bi, and Pb cuprates containing fluorite layers and CuO_2 sheets; (g) mercury cuprates of the type $HgCa_{n-1}Ba_2Cu_nO_{2n+2+\delta}$; and (h) infinite layer cuprates such as $ACuO_2$ (A = Ca, Sr, Ba) and $Ln_{1-x}A_xCuO_2$ (Ln = Nd, Pr; A = Sr, Ba). All these cuprates have holes as charge carriers. The only well established superconducting cuprates with electrons as charge carriers are $Nd_{2-x}M_xCuO_4$ (M = Ce, Th) and related compounds with the T′ structure possessing square-planar CuO_4 units instead of the octahedra in the T structure (Figure 1).

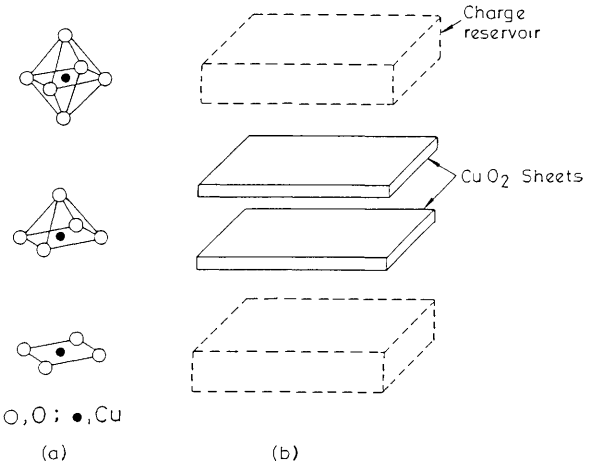

Figure 1 (a) The three types of Cu–O polyhedra found in the superconducting cuprates (b) Schematic representation of cuprates.

* For correspondence

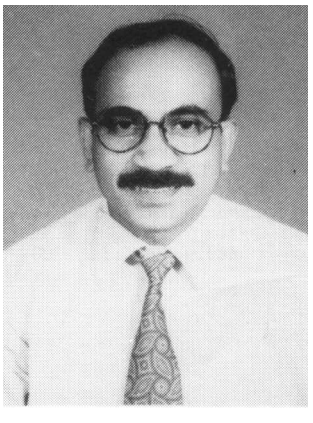

A. K. Ganguli is a scientific officer at the Centre of Excellence in Chemistry at the Indian Institute of Science. He has an M.Sc. degree from the University of Delhi and a Ph.D. degree from the Indian Institute of Science and has carried out post-doctoral work at du Pont and Iowa State University.

C. N. R. Rao is a Professor of Chemical Science at the Indian Institute of Science, and President of the Jawaharalal Nehru Centre for Advanced Scientific Research, Bangalore, India. He is an Honorary Professor of Chemistry at the University of Wales, Cardiff. He was Commonwealth Visiting Professor at the University of Oxford and Nehru Professor at the University of Cambridge. He is a Fellow of the Royal Society, London, Foreign Associate of the U.S. National Academy of Sciences, and Foreign member of several other academies. He is a member of the Pontifical Academy of Sciences and an Honorary Fellow of the Royal Society of Chemistry. He is a recipient of the Marlow Medal of the Faraday Society and the RSC Medal for solid-state chemistry. His main research interests are in solid-state chemistry, spectroscopy, and molecular structure and surface science. He is the author of over 500 research papers and several books in solid state chemistry.

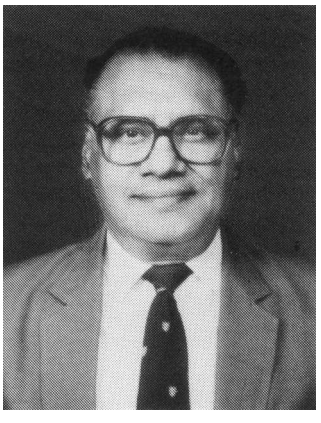

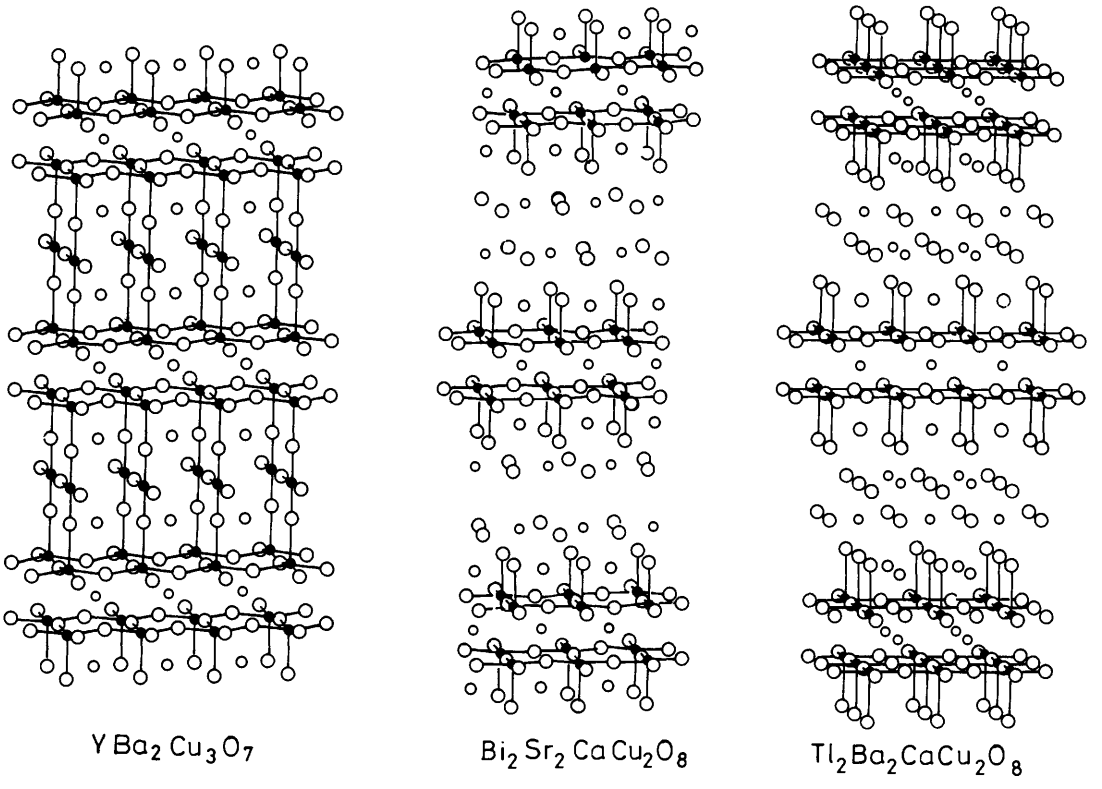

Figure 2 Structures of $YBa_2Cu_3O_7$, $Bi_2CaSr_2Cu_2O_8$, and $Tl_2CaBa_2Cu_2O_8$. Notice the presence of CuO_2 sheets containing CuO_5 square-pyramids. Additionally, there are Cu–O chains in $YBa_2Cu_3O_7$.

Many of the cuprate families have an antiferromagnetic insulator member at one end of the composition (*e.g.* La_2CuO_4 in $La_{2-x}A_xCuO_4$, $YBa_2Cu_3O_6$ in $YBa_2Cu_3O_{7-\delta}$, and $TlYSr_2Cu_2O_7$ in $TlY_{1-x}Ca_xSr_2Cu_2O_{7-\delta}$. What is more interesting is that all the cuprates are at a metal–insulator boundary. Some of them undergo a metal–non-metal transition as a function of composition (*e.g* $Bi_2Ca_{1-x}Y_xSr_2Cu_2O_8$ and $TlY_{1-x}Ca_xSr_2Cu_2O_7$ with change in x).

The cuprates can be described on the basis of certain structural features common to many of them. For example, the structures of $La_{2-x}A_xCaO_4$, $Bi_2(Ca, Sr)_{n+1}Cu_nO_{2n+4}$ and the thallium cuprates can be considered to be intergrowths of oxygen-deficient perovskite layers, $ACuO_{3-x}$, with AO-type rock-salt layers.[7] The cuprates contain different types of Cu–O polyhedra with the hole superconductors necessarily having CuO_5 or CuO_6 units and the electron-superconducting $Nd_{2-x}M_xCuO_4$ containing only CuO_4 square-planar units (Figures 1 and 2). Thus, the essential feature of the cuprates is the presence of CuO_2 sheets with or without apical oxygens. The mobile charge carriers in the cuprates are in the CuO_2 sheets. All the cuprates have charge reservoirs as exemplified by the Cu–O chains in the 123 and 124 cuprates and the TlO, BiO, and HgO layers in the other cuprates. That the CuO_2 sheets are the seat of high-temperature superconductivity is demonstrated by the fact that intercalation of iodine between BiO layers in the bismuth cuprates does not affect the superconducting transition temperature while introduction of fluorite layers between the CuO_2 sheets adversely affects superconductivity. In the different series of cuprates with varying number of CuO_2 sheets studied hitherto, the T_c reaches a maximum when $n = 3$ except in single thallium layer cuprates where the maximum is at $n = 4$. The infinite layered cuprates, where the CuO_2 sheets are separated by alkaline earth and other cations, show T_c's in the 40—110K range.[8] Superconductivity in these materials appears to be due to the presence of Sr–O defect layers corresponding to the insertion of $Sr_3O_{2\pm x}$ blocks.[8]

Based on the interplanar Cu–Cu distances, one can classify cuprates into two categories.[9] In one category, r(Cu–Cu) lies between 3.0 and 3.6 Å with T_c's varying between 50 and 133K and in another it is between ~6 and 12.5 Å encompassing superconductors with lower T_c(< 50K), except $Tl_2Ba_2CuO_6$ and $HgBa_2CuO_{4.065}$ with T_c's of ~90K. In the first category with r(Cu–Cu) < 3.6 Å, the T_c increases as the Cu–Cu distance decreases. In the 2222-type fluorite-based superconductors, there are three copper oxygen sheets, [CuO_2–CuO_δ–CuO_2–fluorite–CuO_2–CuO_δ–CuO_2], each block of three sheets separated by a Ln_2O_2 fluorite layer. The r(Cu–Cu) relevant to these compounds would be the distance between the CuO_2 sheets across the fluorite layer (~ 6.2 Å) and not the distance between two neighbouring sheets. Accordingly, these cuprates exhibit a low T_c(45—50K). It therefore appears that the distance between the CuO_2 sheets is a factor in determining the value of T_c, indicating that there is some interaction between the closely spaced CuO_2 sheets although the cuprates have quasi two-dimensional character.

Oxygen stoichiometry and ordering play a crucial role in determining the structure and properties of cuprates. The dependence of the structure and properties of $YBa_2Cu_3O_{7-\delta}$ on oxygen content has been studied in detail. Thus, $YBa_2Cu_3O_{7-\delta}$ which is orthorhombic ($c \simeq 3\ b$) with a T_c of 90K when $0.0 \lesssim \delta \lesssim 0.25$, assumes another orthorhombic structure ($c \neq 3b$) when $0.3 \lesssim \delta \lesssim 0.4$ with a T_c of 60K. When $\delta = 1.0$, all the oxygens in the CuO chains are depleted and the structure becomes tetragonal and the material is non-superconducting. When $\delta = 0.5$, there is an ordered arrangement of oxygen vacancies with the presence of fully oxidized (O_7) and fully reduced (O_6) chains alternately. The compositions showing 60K superconductivity are metastable and transform to a 124-type phase on heating at low temperatures.[10]

Oxygen-excess La_2CuO_4 is biphasic, consisting of the stoichiometric antiferromagnetic phase and an oxygen-excess superconducting phase.[11] In bismuth cuprates, excess oxygen in the BiO layers gives rise to incommensurate modulation. Modulation-free superconducting bismuth cuprates have been made[12] by replacing one Bi^{3+} by Pb^{2+}. In $HgBa_2CuO_{4+\delta}$ oxygen excess in the Hg plane is necessary to render it superconducting.

3 The Relationship between T_c and the Hole Concentration

As mentioned earlier, a majority of the cuprates have holes as charge carriers These holes are created by the extra positive charge on copper (*e g* Cu^{3+}) or on oxygen (*e g* O^{1-}) The excess positive charge can be represented in terms of the formal valence of copper, which in the absence of holes will be + 2 in the CuO_2 sheets In hole superconducting cuprates, it is generally around + 2 2 In electron superconductors, it would be less than + 2 as expected The actual concentration of holes, n_h, in the CuO_2 sheets in $La_{2-x}A_xCuO_4$, $YBa_2Cu_3O_7$, and Bi cuprates is readily determined by redox titrations In the 123 cuprates, the concentration of mobile holes in the CuO_2 sheets can be delineated from that in the Cu–O chains [13] Determination of n_h in thallium cuprates poses some problems, but in single Tl–O layer cuprates, chemical methods have been developed to obtain reasonable estimates [14] Generally, T_c in a given family of cuprates reaches a maximum value at an optimal value of n_h as shown in Figure 3, the maximum is around $n_h \sim 0\,2$ in most cuprates [15] Notice that the points in the underdoped region in Figure 3 fall close to a straight line Deviations occur in the overdoped region Single layer thallium cuprates also show this behaviour In $Tl_{1-y}Pb_yY_{1-x}Ca_xSr_2Cu_2O_7$ where the substitution of Tl^{3+} by Pb^{4+} has an effect opposite to that due to the substitution of Y^{3+} by Ca^{2+}, the T_c becomes a maximum at an optimal value of $(x-y)$, which is a measure of the hole concentration[16] (Figure 4) By suitably manipulating x and y, the T_c of this system can be increased from 85—90K up to 110K

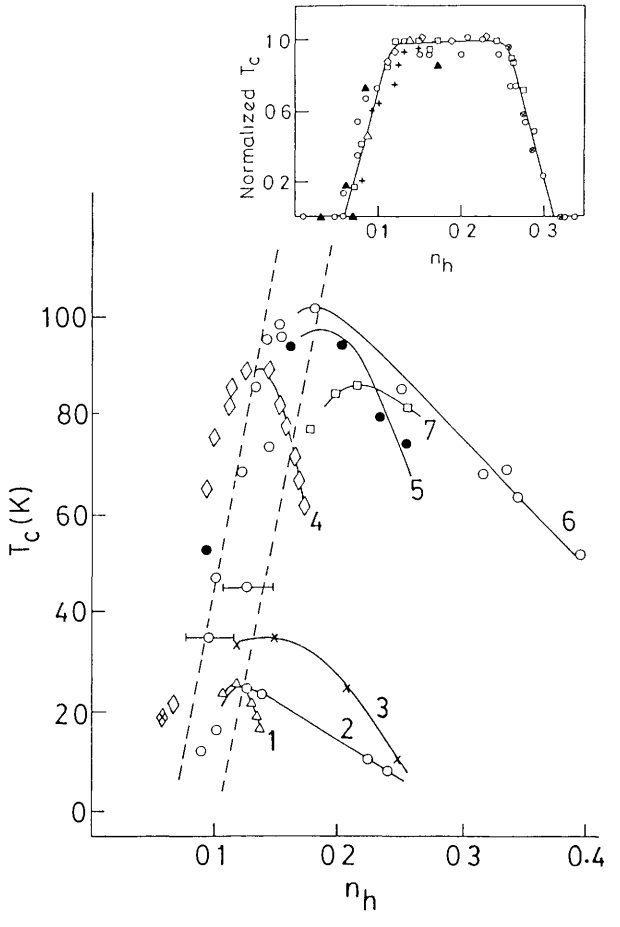

Figure 3 Variation of T_c with hole concentration n_h in superconducting cuprate families (adapted from reference 15) Deviations in overdoped region are similar to those in the plots of muon spin relaxation rate (n_h/m^*) against T_c of Uemura *et al* (*Phys Rev Lett*, 1991, **66**, 2665) 1, 2, 6, and 7, Bi cuprates, 5, 123 cuprates, 3, $La_{2-x}Sr_xCuO_4$, 4, T_c cuprates The variation of normalized T_c with n_h is shown in the inset (from reference 17)

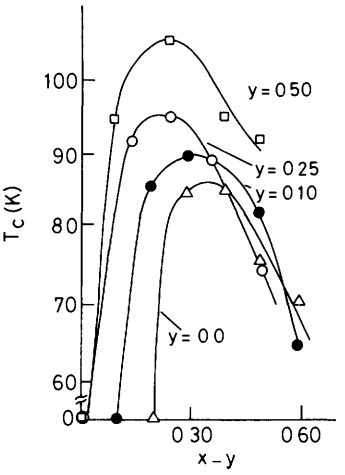

Figure 4 Plots of T_c against the effective hole concentration $(x-y)$ in $Tl_{1-y}Pb_yY_{1-x}Ca_xSr_2Cu_2O_7$ (from reference 16)

Another way of representing the variation[17] of T_c with n_h is to plot the reduced T_c (T_c observed/maximum value of T_c) against n_h as shown in the inset of Figure 3 The ends of the plateau region in this curve correspond to insulating (possibly antiferromagnetic) and metallic regimes of the materials

4 Relation between T_c and the In-plane Cu–O Distance

The Cu–O bonds in the CuO_2 sheets involve an antibonding π interaction and doping with holes reduces the bond distance The in-plane Cu–O bond distance r(Cu–O), therefore reflects the hole concentration and a variation of T_c with r(Cu–O) represents an alternative way of examining the T_c–n_h relationship In cuprates where n_h cannot be determined, as for example in Tl cuprates, the T_c *vs* r(Cu–O) plots show maxima at an optimal distance The value r(Cu–O) is around half that of the a-parameter in most cuprates Whangbo *et al* [18] find three distinct T_c–r(Cu–O) relationships depending on the cation located above and below the CuO_2 sheets, with each exhibiting a T_c maximum at an optimal value of the distance (Figure 5) If we plot the reduced T_c against r(Cu–O), we get the curves shown in Figure 6 where the highest T_c values occur in the 1 89—1 94 Å

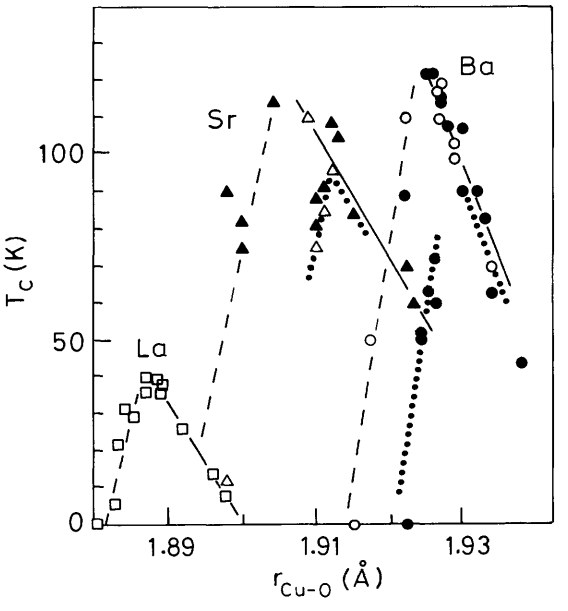

Figure 5 Variation of T_c with in-plane Cu–O distances in various families of cuprates (from reference 18)

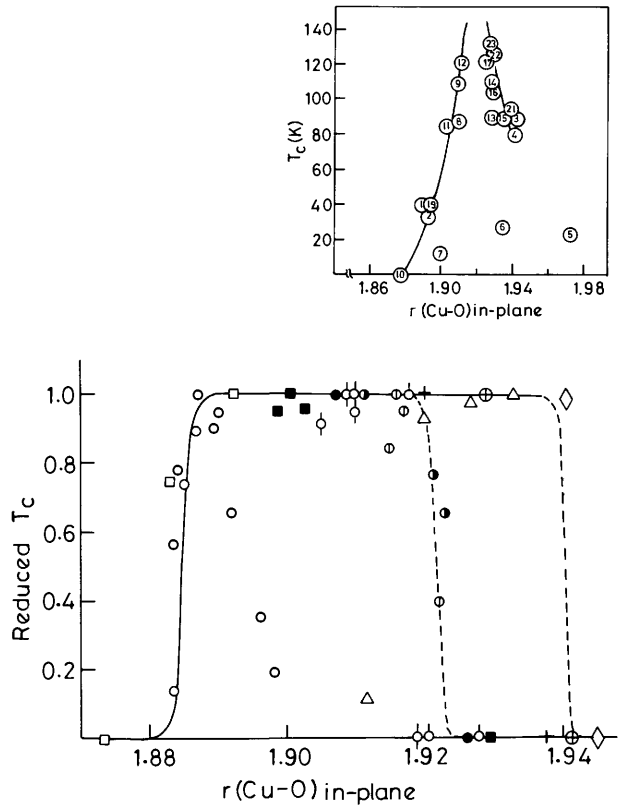

Figure 6 Plot of reduced T_c with in-plane r(Cu–O) distance: $La_{2-x}Sr_xCuO_4$ (open circles), $YBa_2Cu_3O_{7-\delta}$ (circles with cross), Bi_2 (Ca, Y, Sr)$_3Cu_2O_8$ (half-shaded circles), $Bi_2Ca_{1-x}Y_xSr_2Cu_2O_8$ (circles with a line in the centre), modulation-free Bi-cuprates (filled squares), $TlSr_{2-x}La_xCuO_5$ (open squares), $Tl_2Ba_{2-x}Sr_xCuO_6$ (open triangles), $TlCa_{1-x}Y_xBa_2Cu_2O_7$ (crosses), $TlCa_{1-x}Ln_xSr_2Cu_2O_7$ (circles with one line on top), and $Tl_{0.5}Pb_{0.5}Ca_{1-x}Y_xSr_2Cu_2O_7$ (circles with lines above and below), $Pb_2Sr_2Y_{1-x}Ca_xCu_3O_{8+\delta}$ (filled circles), $HgBa_2CuO_{4+\delta}$ (open diamonds). Inset shows the variation of T_c with the in-plane Cu–O distance where only the cuprate compositions showing the maximum T_c in each family are taken into account. (1) $La_{1.85}Sr_{0.15}CuO_4$. (2) $La_{1.85}Ba_{0.15}CuO_4$. (3) $YBa_2Cu_3O_{6.91}$. (4) $YBa_2Cu_4O_8$. (5) $Nd_{1.85}Ce_{0.15}CuO_4$. (6) $Nd_{1.4}Ce_{0.2}Sr_{0.4}CuO_4$. (7) $Bi_2Sr_2CuO_6$. (8) $Bi_2CaSr_2Cu_2O_8$. (9) $Bi_2Ca_2Sr_2Cu_3O_{10}$. (10) $Tl_{0.5}Pb_{0.5}Sr_2CuO_5$. (11) $Tl_{0.5}Pb_{0.5}CaSr_2Cu_2O_7$. (12) $Tl_{0.5}Pb_{0.5}Ca_2Sr_2Cu_3O_9$. (13) $TlCaBa_2Cu_2O_7$. (14) $TlCa_2Ba_2Cu_3O_9$. (15) $Tl_2Ba_2CuO_6$. (16) $Tl_2CaBa_2Cu_2O_8$. (17) $Tl_2Ca_2Ba_2Cu_3O_{10}$. (18) $Tl_2Ca_3Ba_2Cu_4O_{12}$. (19) $TlSrLaCuO_5$. (2) $TlCa_{0.5}La_{0.5}Sr_2Cu_2O_7$. (21) $HgBa_2CuO_{4.065}$. (22) $HgCaBa_2Cu_2O_{6.22}$. (23) $HgCa_2Ba_2Cu_3O_{8.41}$.

range. When r(Cu–O) < 1.88 Å, the material is metallic; those with r(Cu–O) > 1.94 Å are certainly insulating, but there are different insulating boundaries for the different cation families, somewhat like in Figure 5. However, if we consider only the maximum T_c value in each cuprate family and the corresponding r(Cu–O), we get the curve shown in the inset of Figure 6 which peaks at $r \approx 1.92$ Å. $Bi_2Sr_2CuO_6$ with a T_c of 12K would not fall on the curve, but $Bi_2Sr_{2-x}La_xCuO_{6+\delta}$ with a T_c of 30K would.

5 The Relationship between T_c and the Apical Cu–O Distance

All the cuprates which are hole superconductors have apical oxygens which act as the link between the charge reservoirs and the CuO_2 sheets. (Note that electron superconductors such as $Nd_{2-x}Ce_xCuO_4$ contain only CuO_4 units without apical oxygens.) In $YBa_2Cu_3O_{7-\delta}$, the T_c–r(Cu2–O1) relationship (Figures 7a and b) mirrors the T_c–δ relationship.[19] In $YBa_2Cu_4O_8$, the T_c increases with pressure from 80K to 90K, as the apical Cu–O distance decreases[20] (Figure 7c). We have sought to find relationships between T_c and apical Cu–O distance in

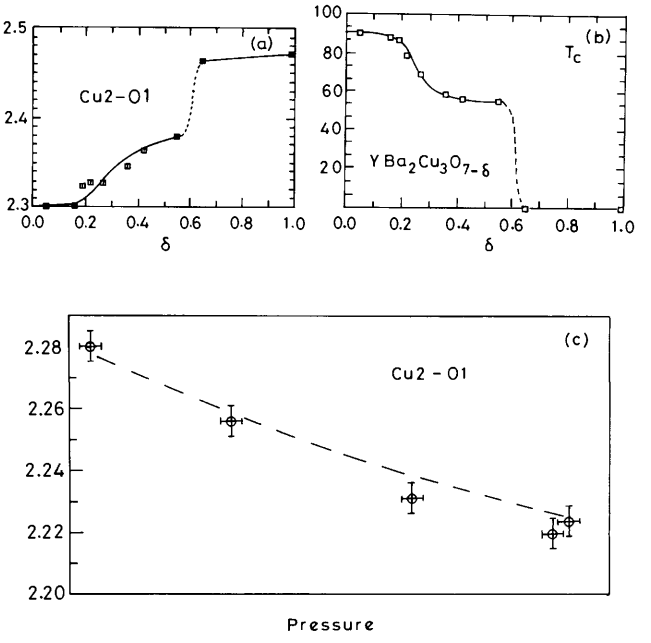

Figure 7 Variation of (a) the apical Cu–O distance with δ in $YBa_2Cu_3O_{7-\delta}$ (b) T_c with δ and (c) variation of the Cu–O apical distance with pressure in $YBa_2Cu_4O_8$ as shown by the points (the dashed line is obtained by the oxidation of $YBa_2Cu_3O_{7-\delta}$) (from references 19 and 20).

different cuprate families (Figure 8). Within a series of cuprates with varying number of CuO_2 sheets, (*e.g.*, $TlCa_{n-1}Ba_2Cu_nO_{2n+3}$), the apical (Cu–O) distance decreases with the increase in n while T_c increases linearly with the decrease in the apical distance. The slope of the T_c *vs.* the apical Cu–O distance plot is nearly the same in $TlCa_{n-1}Ba_2Cu_nO_{2n+3}$, $Tl_{0.5}Pb_{0.5}Ca_{n-1}Sr_2Cu_nO_{2n+3}$, and $HgCa_{n-1}Ba_2Cu_nO_{2n+3}$, all of them having a single rock-salt layer (TlO, $Tl_{0.5}Pb_{0.5}O$, or HgO_δ). The $Tl_2Ca_{n-1}Ba_2Cu_nO_{2n+4}$ family also shows increasing T_c with the decrease in the apical Cu–O distance, but with a different slope. The mercury-based superconductors have larger apical distances compared to the other cuprates and they also show a large pressure dependence of T_c. Interestingly, if we consider the maximum T_c points at the top of the plots for the different

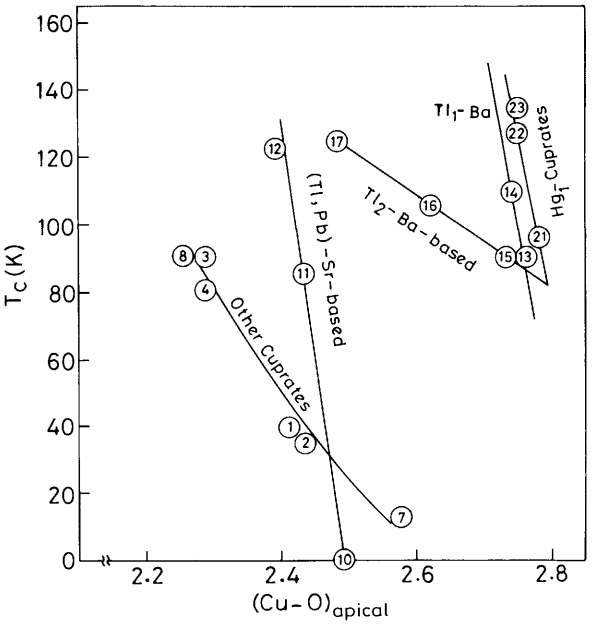

Figure 8 Variation of T_c with the apical Cu–O distance in cuprate superconductors.

groups of cuprates in Figure 8, we see that the T_c increases with the increase in the apical Cu–O distance.

6 Covalency of the Charge Reservoir

All the superconducting cuprates have charge reservoirs and any damage to these reservoirs adversely affects superconductivity. The nature of the charge reservoir determines the carrier concentration and the ease of charge-transfer to the CuO_2 sheets. Covalent charge reservoirs can redistribute charge effectively through the apical oxygen of the CuO_5 square pyramids giving rise to high T_c's. Ionic charge reservoirs, on the other hand, would be less flexible with regard to the charge states and do not favour high T_c's. Structural mismatch as well as disorder in the reservoirs also adversely affect the superconducting properties. The covalency of the Hg–O bond could be related to the high T_c of Hg cuprates.

The effect of covalency of the charge reservoir is clearly seen in $Tl_{0.5}Pb_{0.5}Sr_2Y_{1-x}Ca_xCu_2O_7$ which shows a T_c of 110K at an optimal x value, the material being an insulator when $x = 0.0$. The a parameter decreases with the increase in x, because the population of the antibonding Cu $3d_{x^2-y^2}$ orbitals decreases with the increase in x, causing a strengthening of the Cu–O bond. The puckering of the CuO_2 sheets decreases with increasing hole concentration. The displacement of the apical oxygen is around 0.06Å when $x = 1.0$ and 0.20Å when $x = 0.0$. An increase in Y content (increased electron population), however, increases the puckering and pulls the apical oxygen away from the base of the pyramid.

7 The Relationship between T_c and Madelung Potentials

The role of the Madelung site potential in the hole conductivity of the cuprate superconductors was first pointed out by Torrance and Metzger.[21] Two classes of cuprates can be delineated depending on the value of ΔV_M which is the difference in Madelung site potential for a hole on a Cu site and that on an oxygen site. Those with high ΔV_M ($\geq$47eV) are metallic and superconducting; those with lower ΔV_M are semiconducting with localized holes. It is possible to define a term ΔV_A which is the difference in the Madelung site potentials for a hole between the apex and the in-plane oxygen atoms and provides a measure of the position of the energy level of the p_z-orbital on the apical oxygens.[22] When the maximum values of T_c of hole-doped superconductors are plotted against ΔV_A (Figure 9), one finds that nearly all the cuprates are located on a curve (with some width), the cuprates with large ΔV_A exhibiting high T_c's. It appears that the energy level of the apical oxygen plays a significant role in the electronic states of the doped holes,

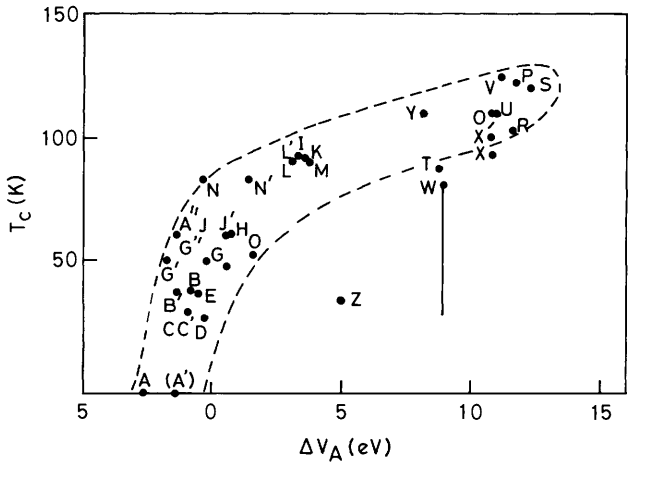

Figure 9 Variation of T_c with ΔV_A. See reference 22 for the explanation of the letter symbols.

thereby affecting the T_c. The correlation probably owes its origin to the stability of local singlet states made up of two holes in the Cu $3d_{x^2-y^2}$ and O $2p$ orbitals in the CuO_2 sheet. The local singlet is well defined and stable when the energy level of the apical oxygen atom is sufficiently high. A comparison of the correlations of T_c with ΔV_A and ΔV_M indicates that ΔV_A scales better with T_c.

It is instructive to correlate T_c simultaneously with ΔV_M and the in-plane Cu–O bond length, d_p, in the CuO_2 planes. The maximum T_c for each cuprate is shown in the d_p *vs.* ΔV_M plot[23] in Figure 10. The data points are confined to a narrow strip running from the top left (high d_p and low ΔV_M) to the bottom right corner (low d_p and high ΔV_M). The T_c value increases as we go from right to left (larger to smaller value of ΔV_M) or from top to bottom (from higher d_p to lower d_p). An important observation is that T_c changes to a small extent as one goes from the top left to bottom right (d_p decreasing and ΔV_M increasing) while T_c increases drastically when traversing from the top right to bottom left of the map (both d_p and ΔV_M decreasing). Clearly, the T_c is governed by both ΔV_M and d_p. It appears that the difference in T_c is a result of the difference in internal stress of the crystal (high T_c when the CuO_2 planes are under compression and low T_c when they are strained).

8 The Relationship between Bond Valence Sums and T_c

The bond-valence sum is a measure of the total charge on an atom in a structure. Its value changes with oxygen doping, cation substitution, or applied pressure indicating the occurrence of charge transfer within the structure. One defines, $V_- = 2 + V_{Cu2} - V_{O2} - V_{O3}$ where V_- is the total excesss charge in the planes (O2 and O3 are the oxygens in the plane) and $V_+ = 6 - V_{Cu2} - V_{O2} - V_{O3}$. The T_c *vs.* V_- plot for $YBa_2Cu_3O_{7-\delta}$ is similar to the T_c vs. δ plot; the plot of T_c against V_+ is linear[24] (Figure 11).

9 The Importance of the Cu–O Charge-Transfer Energy

One of the unique features of the cuprates is the relatively small Cu–O charge-transfer energy. It is therefore of significance to relate this property with superconductivity. *X*-Ray photoemission spectra of cuprates in the Cu $2p_{3/2}$ region show a characteristic two-peak feature. The peak around 933 eV (main peak) is due to a final state with primarily $3d^{10}$ character, while the peak of weaker intensity at about 941 eV binding energy is mainly due to a $3d^9$ final state (satellite). Model calculations of the Cu $2p$ core-level photoemission within a CuO_4 square-planar cluster show that the I_s/I_m ratio (relative intensity of the satellite to the main peak) is related to Δ/t_{pd} where Δ is the charge-transfer excitation energy and t_{pd} is the hybridization strength between the Cu $3d$ and O $2p$ orbitals. Thus, any relationship between the experimentally observed I_s/I_m ratio with n_h would suggest a link between n_h (T_c) and the Δ/t_{pd} ratio. It is indeed found that the I_s/I_m ratio is related to the hole concentration n_h in many of the superconducting cuprates.[25]

In Figure 12(a), we show the relative intensity of the satellite (I_s/I_m) as a function of x in $La_{2-x}Sr_xCuO_4$. In the same plot, we also show the variation of the experimentally determined hole concentration with x in this series. The inset of Figure 12(a) shows the dependence of T_c on n_h exhibiting a maximum around $n_h = 0.15$. We see that the value of I_s/I_m decreases markedly with increasing x until about 0.3, after which it changes slope. What is significant is that I_s/I_m decreases as the hole concentration increases. In Figure 12(b) we show the variation of n_h and I_s/I_m with x in $BiPbSr_2Y_{1-x}Cu_2O_8$. In the inset we show the variation of T_c with n_h. Here also we see that the I_s/I_m ratio decreases as the hole concentration increases. Figure 13 shows how in three series of high T_c cuprates, the I_s/I_m ratio decreases monotonically with the increase in magnitude of hole doping. The

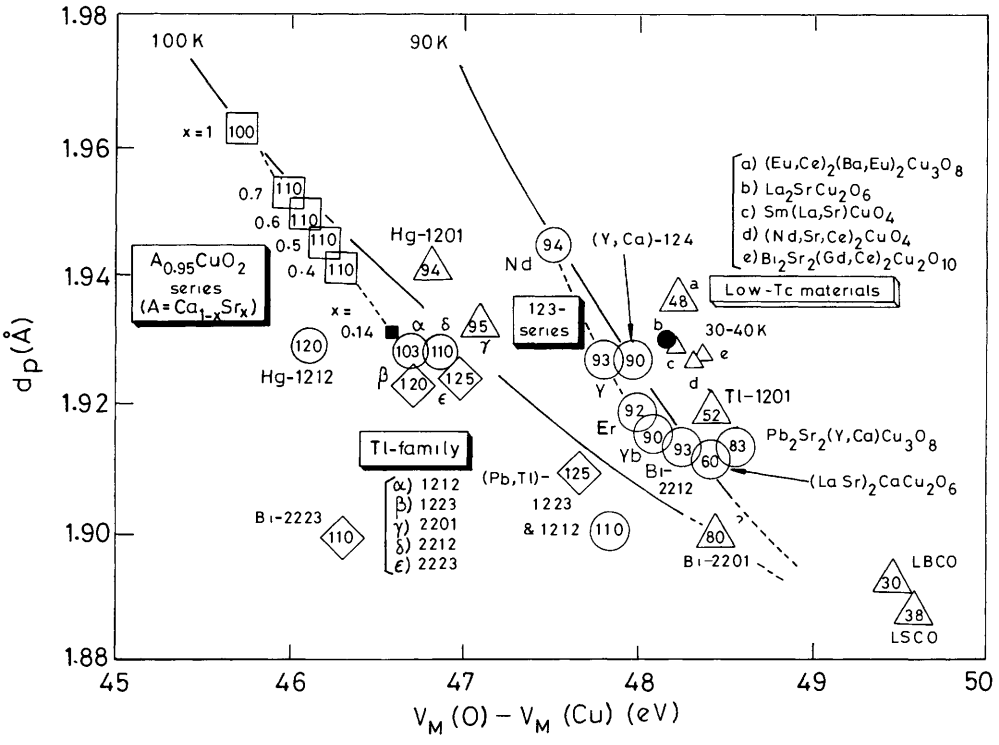

Figure 10 Plot of d_p *vs.* ΔV_M showing region of high T_c and low T_c superconductors (from reference 23).

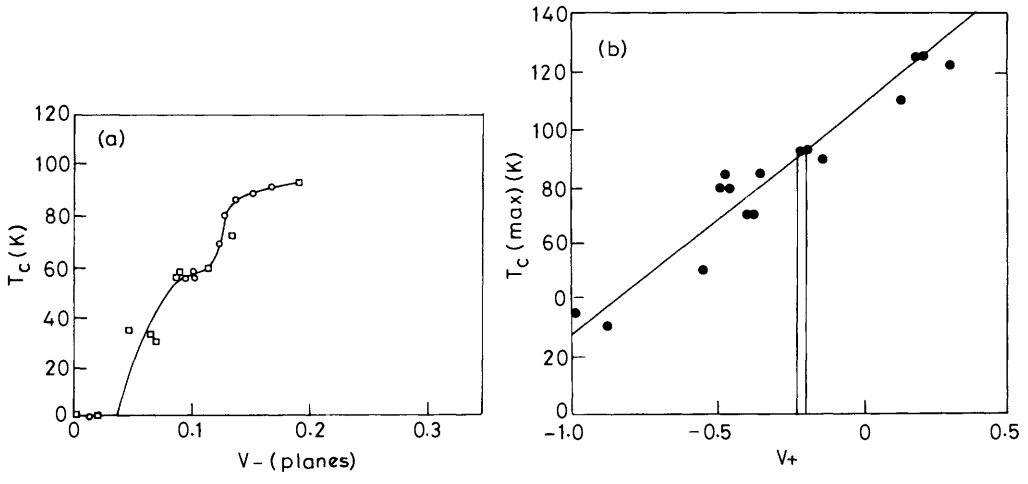

Figure 11 Variation of (a) T_c with V_- (see text) and (b) T_c with V_+ for $YBa_2Cu_3O_{7-\delta}$ (from reference 24).

variation is smooth across the insulator–superconductor–metal boundaries. Calculations show that the I_s/I_m ratio increases with the Δ/t_{pd} ratio in the cuprates. Accordingly, at a given n_h value where the T_c is maximum, increasing I_s/I_m is accompanied by an increase in T_c. Thus, $Bi_2Ca_{1-x}Ln_xSr_2Cu_2O_{8+\delta}$ exhibits the highest T_c of around 100K while $La_{2-x}Sr_xCuO_4$ has the lowest T_c value. The observation of a maximum T_c around an optimal value of n_h or Cu–O distance can therefore be traced to the optimal Δ/t_{pd} value or of the Cu–O charge-transfer energy.

10 Concluding Remarks

We have discussed several interesting correlations between the superconducting transition temperature and some of the crucial structural and electronic parameters. These correlations along with the structural commonalities in the cuprates show how superconductivity is intimately connected with the structural chemistry of these materials. They may also suggest many other relationships, some of which may be even more significant.

Acknowledgement. The authors thank the Science Office of the European Union, the Department of Science and Technology, and the University Grants Commission for support of this research.

7 References

1 C. N. R. Rao, K. J. Rao, and J. Gopalakrishnan, *Ann. Rep. Prog. Chem., Sect C*, 1985, **82**, 193.
2 J. Bednorz and K. A. Müller, *Z. Phys.*, 1986, **B64**, 189.
3 B. Raveau, C. Michel, M. Hervieu, and D. Groult, 'Crystal Chemistry of High T_c Superconducting Copper Oxides', Springer-Verlag, Berlin, 1991.
4 'Chemistry of High-Temperature Superconductors', ed. C. N. R. Rao, World Scientific, Singapore, 1991.

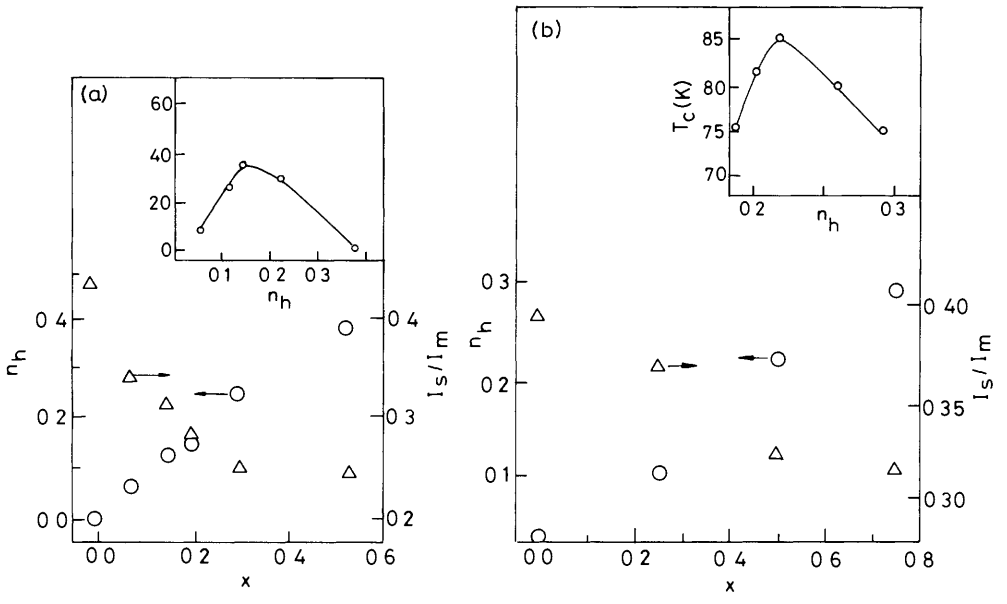

Figure 12 (a) Variation of I_S/I_M ratio with x in $La_{2-x}Sr_xCuO_4$ (b) Also shown is the variation of n_h with x and I_S/I_M and n_h with x in $BiPbSr_2Y_{1-x}Ca_xCu_2O_8$ (from reference 25)

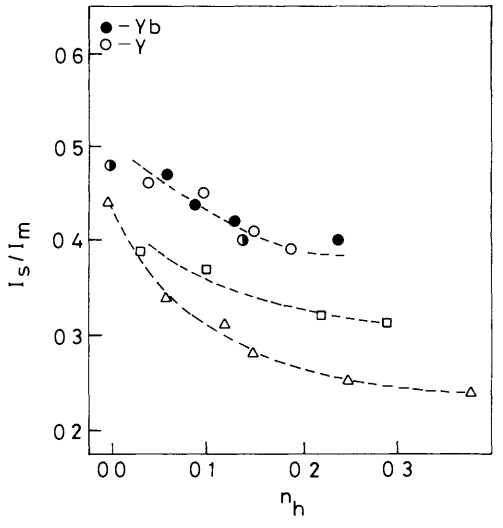

Figure 13 Variation of the I_S/I_M ratio with hole concentration (n_h) $La_{2-x}Sr_xCuO_4$ (triangles), $BiPbSr_2Y_{1-x}Ca_xCu_2O_\delta$ (squares), and $Bi_2Ca_{1-x}L_xSr_2CuO_2O_8$ (circles) (from reference 25)

5 M Nunez-Regueiro, J L Tholence, E V Antipov, J J Capponi, and M Marezio, *Science*, 1993, **262**, 976
6 A R Armstrong and P P Edwards, *Ann Rep Prog Chem Sect C*, 1991, **88**, 259
7 C N R Rao, *Philos Trans R Soc London*, 1991, **A336**, 595, 106
8 H Zhang, Y Y Wang, V P Dravid, L D Marks, P D Han, D A Payne, P G Radaelli, and J D Jorgensen, *Nature*, 1994, **370**, 352, and references therein
9 H Nobumasa, K Shimizu, and T Kawai, *Physica C*, 1990, **167**, 515
10 R Nagarajan and C N R Rao, *J Solid State Chem*, 1993, **103**, 533
11 J D Jorgensen, *Physics Today*, 1991, **44**, 34
12 V Manivannan, J Gopalakrishnan, and C N R Rao, *Phys Rev B* 1991, **43**, 8686
13 R Nagarajan and C N R Rao, *J Mater Chem*, 1993, **3**, 969
14 C N R Rao in 'Thallium-based High Temperature Superconductors', ed A M Hermann and J V Yakhmi, Marcel Dekker, New York, 1994
15 C N R Rao, J Gopalakrishnan, A K Santra, and V Manivannan, *Physica C*, 1991, **174**, 11
16 R Vijayaraghavan, N Rangavittal, G U Kulkarni, E Grantscharova, T N Guru Row, and C N R Rao, *Physica C*, 1991, **179**, 183
17 H Zhang and H Sato, *Phys Rev Lett*, 1993, **70**, 1697
18 M H Whangbo, D B Kang, and C C Torardi, *Physica C*, 1989, **158**, 371
19 R J Cava, A W Hewat, E A Hewat, B Batlogg, M Marezio, K B Rabe, J J Krajewski, W F Peck, and L W Rupp, *Physica C*, 1990, **165**, 419
20 R J Nelmses, E Loveday, E Kaldis, and J Karpinski, *Physica C*, 1992, **172**, 311
21 J B Torrance and R M Metzger, *Phys Rev Lett*, 1989, **63**, 1515
22 Y Ohta, T Tohyama, and S Maekawa, *Physica C*, 1990, **167**, 515
23 M Muroi, *Physica C*, 1994, **219**, 129
24 J L Tallon and G V M Williams, *J Less Common Metals*, 1990, **164—165**, 60
25 A K Santra, D D Sarma, and C N R Rao, *Phys Rev B*, 1991, **43**, 5612